Journal of the American College of Cardiology
© 2010 by the American College of Cardiology Foundation
Published by Elsevier Inc.

Vol. 55, No. 2, 2010
ISSN 0735-1097/10/$36.00
doi:10.1016/j.jacc.2009.08.041

PRE-CLINICAL RESEARCH

Growth Differentiation Factor 5 Regulates Cardiac Repair After Myocardial Infarction

Syed H. E. Zaidi, PHD,*†§ Qingling Huang, PHD,§ Abdul Momen, MD,§ Ali Riazi, PHD,‖ Mansoor Husain, MD*†‡

Toronto, Ontario, Canada

Objectives The aim of this study was to examine the function of the bone morphogenic protein growth differentiation factor 5 (Gdf5) in a mouse model of myocardial infarction (MI).

Background The Gdf5 has been implicated in skeletal development, but a potential role in the heart had not been studied.

Methods The Gdf5-knockout (KO) and wild-type (WT) mice were subjected to permanent left anterior descending coronary artery (LAD) ligation. Cardiac pathology, function, gene expression levels, and signaling pathways downstream of Gdf5 were examined. Effects of recombinant Gdf5 (rGdf5) were tested in primary cardiac cell cultures.

Results The WT mice showed increased cardiac Gdf5 levels after MI, with increased expression in peri-infarct cardiomyocytes and myofibroblasts. At 1 and 7 days after MI, no differences were observed in ischemic or infarct areas between WT and Gdf5-KO mice. However, by 28 days after MI, Gdf5-KO mice exhibited increased infarct scar expansion and thinning with decreased arteriolar density compared with WT. The Gdf5-KO hearts also displayed increased left ventricular dilation, with decreased contractility after MI. At 4 days after MI, Gdf5-KO mice exhibited increased cardiomyocyte apoptosis and decreased expression of anti-apoptotic genes Bcl2 and Bcl-xL compared with WT. Unexpectedly, Gdf5-KO hearts displayed increased Smad 1/5/8 phosphorylation but decreased p38-mitogen-activated protein kinase (MAPK) phosphorylation versus WT. The latter was associated with increased collagen gene (Col1a1, Col3a1) expression and fibrosis. In cultures, rGdf5 induced p38-MAPK phosphorylation in cardiac fibroblasts and Smad-dependent increases in Bcl2 and Bcl-xL in cardiomyocytes.

Conclusions Increased expression of Gdf5 after MI limits infarct scar expansion in vivo. These effects might be mediated by Gdf5-induced p38-MAPK signaling in fibroblasts and Gdf5-driven Smad-dependent pro-survival signaling in cardiomyocytes. (J Am Coll Cardiol 2010;55:135–43) © 2010 by the American College of Cardiology Foundation

Growth differentiation factor 5 (Gdf5), also known as bone morphogenetic protein (BMP) 14, is a secreted morphogen of the transforming growth factor-beta super-family, conferring signaling by activation of Smad 1/5/8 or mitogen-activated protein kinase (p38-MAPK) (1,2). The Gdf5 is one of the few morphogenetic proteins that interact with both type 2 BMP and activin receptors with equivalent affinities (3). This ability of Gdf5 and its persistent expression in postnatal tissues posit a potentially important role.

From the *Division of Cardiology, University Health Network, Toronto, Ontario, Canada; and †Department of Medicine and ‡Heart & Stroke Richard Lewar Centre of Excellence in Cardiovascular Research, University of Toronto, Toronto, Ontario, Canada; §McEwen Centre for Regenerative Medicine, Toronto General Hospital Research Institute, Toronto, Ontario, Canada; and the ‖Labatt Family Heart Centre, Hospital for Sick Children, Toronto, Ontario, Canada. This work was supported by grants from the Heart & Stroke Foundation of Ontario (HSFO) (NA5808) and Toronto General Hospital Foundation to Dr. Zaidi, and grants from the Canadian Institutes of Health Research (MOP117801) and HSFO (CI: 5503) to Dr. Husain.

Manuscript received May 11, 2009; revised manuscript received July 15, 2009, accepted August 3, 2009.

During development, Gdf5 is expressed in several tissues including the heart (4–6). Studies in vitro suggest that Gdf5 has effects on angiogenesis (7,8), apoptosis (9), cell survival (6), differentiation (10), and migration (7). Although Gdf5 expression continues into adulthood in some tissues (4), its role in the heart had not been studied. Mutations in Gdf5 produce skeletal disorders in humans and in mice (4). Gdf5-deficient mice exhibit reduced revascularization and delayed healing after tendon injury (11). Given these findings, we hypothesized that Gdf5 might influence remodeling and repair processes in the heart.

See page 144

Here we show that Gdf5 protein and its receptors are expressed in the adult mouse heart and that Gdf5 levels are elevated after myocardial infarction (MI). To study the role of Gdf5 in cardiac repair, we compared the structure and function of Gdf5-knockout (KO) and wild-type (WT) hearts after left anterior descending coronary artery (LAD) ligation. To exam-

JACC Vol. 55, No. 2, 2010
January 12, 2010:135–43

Abbreviations and Acronyms

AW = anterior wall
ERK = extracellular signal regulated kinase
Gdf5 = growth differentiation factor 5
ID1 = inhibitor of differentiation 1
LAD = left anterior descending coronary artery
LV = left ventricle/ventricular
MAPK = mitogen-activated protein kinase
MI = myocardial infarction
MMP = matrix metalloproteinase
mRNA = messenger ribonucleic acid
KO = knockout
rGdf5 = recombinant growth differentiation factor 5
RNA = ribonucleic acid
RNAi = ribonucleic acid interference
RT-PCR = reverse-transcriptase polymerase chain reaction
SM = smooth muscle
TUNEL = terminal deoxynucleotidyl transferase (TdT)-mediated dUTP nick end labeling
WT = wild-type

ine the mechanisms underlying abnormal cardiac repair in Gdf5-KO mice, we studied Smad 1/5/8 and p38-MAPK signaling, collagen gene expression, fibrosis, apoptosis, and vascularization. In addition, we examined the effects of Gdf5 on survival of neonatal cardiomyocytes. This is the first report of the effects of Gdf5 deficiency in particular and a BMP family member in general on cardiac repair.

Methods

Animals. The C57Bl6 mice and mice heterozygous for the Gdf5 (bp^{3J} allele) were purchased from Jackson Laboratory (Bar Harbor, Maine). Heterozygous mice were crossed to obtain homozygous KO and WT littermates.

Surgery and hemodynamic procedures. Mice (8 to 12 weeks of age) were subjected to LAD ligation or sham surgery according to protocols approved by our institutional Animal Care Committee. Experimental procedures for this model are detailed elsewhere (12). For in vivo hemodynamic measurements, mice were anesthetized with 1% isoflurane, and the right carotid artery was cannulated with a micromanometer catheter (Millar Instruments, Houston, Texas). Heart rate, aortic blood pressures, left ventricular (LV) systolic pressure, and peak positive and negative first derivatives of the LV pressure (±dP/dt) were recorded.

Reverse-transcriptase polymerase chain reaction. Ribonucleic acid (RNA) was isolated and reverse-transcribed with the SuperScript III kit (Invitrogen, Burlington, Ontario, Canada). Quantitative real-time polymerase chain reaction (PCR) was performed with SYBR green as per the manufacturer (Applied Biosystems, Streetsville, Ontario, Canada). Real-time data were normalized to glyceraldehyde-3-phosphate dehydrogenase complementary deoxyribonucleic acid. Primer sequences are listed in Supplementary Table A.

Histology, immunohistochemistry, and Western blot. Hearts were fixed in 10% formalin, paraffin-embedded, sectioned (5 μm), and stained with hematoxylin and eosin or trichrome. Images were captured and analyzed by Image J software (National Institute of Health). Infarct area, transmurality, and expansion index were calculated as described (13). Antibody against Gdf5 (R&D Systems, Minneapolis, Minnesota; and Santa Cruz Biotechnology, Santa Cruz, California), smooth muscle (SM)-alpha-actin (Dako, Mississauga, Ontario, Canada), activated caspase 3, phosphorylated Smad 1/5/8, phosphorylated and total p38-MAPK, extracellular signal regulated kinase (ERK)1/2 and c-jun N-terminal kinase, Bcl2 and Bcl-xL (Cell Signaling Technology, Danvers, Massachusetts), total Smad 1/5/8 and inhibitor of differentiation 1 (ID1) (Santa Cruz Biotechnology, Santa Cruz, California), HRP-conjugated secondary antibodies (Bio-Rad, Mississauga, Ontario, Canada), and the Vectastain kit (Vector Laboratories, Burlington, Ontario, Canada) were employed for immunohistochemistry and/or Western blot. Myocardial fibrosis was assessed by trichrome as described (12).

Cell culture. Neonatal mouse cardiac fibroblasts and cardiomyocytes were prepared as described (14,15) (Supplementary Fig. 1). Cells were cultured in Dulbecco's modified Eagle's media/F12 media containing 10% serum. Passage 2 fibroblasts were kept in 0.1% serum containing medium for 38 h and stimulated with recombinant Gdf5 (rGdf5, R&D Systems) at a concentration of 250 ng/ml. Cardiomyocytes were treated with buffer or rGdf5 at a concentration 250 ng/ml. Terminal deoxynucleotidyl transferase (TdT)-mediated dUTP nick end labeling (TUNEL) was performed with the CardioTACS kit (R&D Systems).

Ribonucleic acid interference (RNAi). Stealth RNAi against mouse Gdf5, Smad 4, p38-MAPK (Mapk14), negative control, BlockiT alexa Fluor, and lipofectamine 2000 were purchased from Invitrogen. The RNAi were transfected at a final concentration of 20 nmol/l as described by the manufacturer, and gene expression was assessed by quantitative real time reverse-transcriptase polymerase chain reaction (RT-PCR).

Statistical methods. Data for Gdf5 expression, ventricular to body weight ratios, and vascularity were analyzed by 2-way analysis of variance followed by Bonferroni test for multiple comparisons among groups. When only 2 groups were compared, the Student *t* test was applied. Collagen expression data were analyzed by single factor analysis of variance followed by Student *t* test. All values shown are mean ± SEM.

Results

Adult mouse heart expresses Gdf5 and its receptors. To conclusively establish that Gdf5 is expressed in the heart, RT-PCR was performed on messenger ribonucleic acid (mRNA) from whole adult mouse hearts (n = 3). The amplified product was sequenced to confirm Gdf5 expression (Fig. 1A). Similarly, RT-PCR was used to confirm the expression of BMP and activin receptors through which Gdf5 transduces its signals. Both type 1 (Bmpr1b) and type 2 (Bmpr2, Acvr2a, Acvr2b) receptors were expressed.

Cardiac Gdf5 expression is increased after MI. Anterior walls (AWs) (infarct) and posterior walls (PW) (noninfarct) of the LV were dissected for RNA extraction. The RT-PCR revealed serial increases in Gdf5 mRNA levels in the infarct-containing AW. To quantify this, real-time quantitative RT-PCR was also performed. Compared with sham and nonsur-

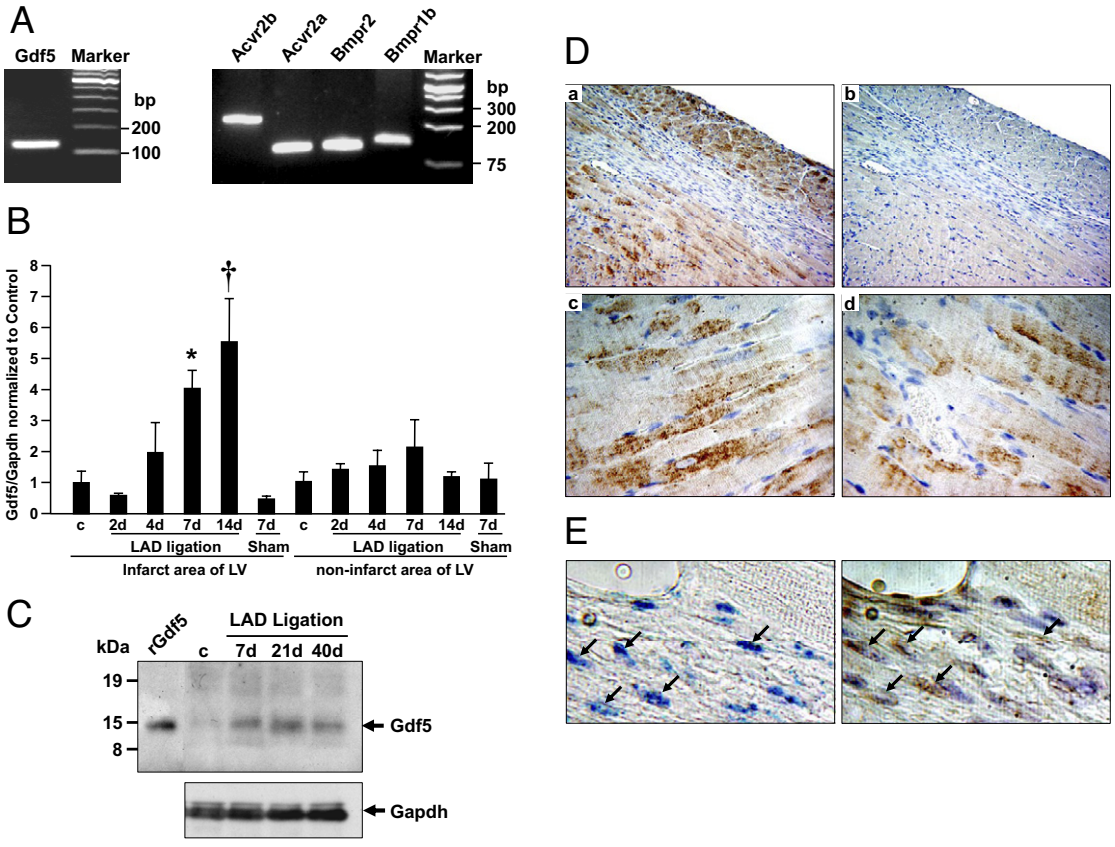

Figure 1 **Gdf5 Levels Are Regulated After MI**

(A) Reverse-transcriptase polymerase chain reaction–defined expression of growth differentiation factor 5 (Gdf5) and bone morphogenetic protein (BMP) and activin receptors in the adult mouse heart. **(B)** Real-time quantification of Gdf5 messenger ribonucleic acid (mRNA) expression in the anterior walls (infarct) and posterior walls (noninfarct). All data were normalized to glyceraldehyde-3-phosphate dehydrogenase (Gapdh) mRNA **Bar "c"** represents noninfarcted control. All data are given as mean ± SEM (n = 3 mice/bar). Data were compared by 2-way analysis of variance (ANOVA) ($p < 0.001$) followed by Bonferroni test for multiple comparisons. **(C)** Elevated cardiac Gdf5 protein levels are evident 7, 21, and 40 days after myocardial infarction (MI). Recombinant Gdf5 (rGdf5) is a positive control. **(D)** Immunohistochemistry shows elevated Gdf5 protein expression in peri-infarct cardiomyocytes at 14 days after MI **(a, c, and d)**. IgG control was used in **panel b**. **Panels c and d** are higher magnifications of the Gdf5-stained section. **(E)** The Gdf5 expression **(brown staining, right panel)** was also observed in smooth muscle cell-alpha actin-positive cardiac myofibroblasts **(blue staining, left panel)**. The **right panel** is counterstained with hematoxylin **(blue)** to visualize nuclei. **Arrows** denote cells which are stained for smooth muscle cell-alpha actin. *$p < 0.025$; †$p < 0.003$. LAD = left anterior descending coronary artery; LV = left ventricle.

gery control subjects, Gdf5 mRNA levels were elevated at 7 and 14 days after MI (Fig. 1B). The Gdf5 mRNA levels at 7 and 14 days after MI were 8.5- and 11.6-fold higher, respectively, in the AW of infarcted mice as compared with the AW of 7-day sham-operated control subjects ($p < 0.025$). Increased cardiac Gdf5 protein expression after MI was confirmed by Western blot (Fig. 1C), which revealed that Gdf5 protein levels remained elevated up to 40 days after MI (reaching maximum levels at 21 days). Immunohistochemistry at 14 days showed elevated Gdf5 expression in cardiomyocytes (Fig. 1D) and myofibroblasts (Fig. 1E) in the peri-infarct areas of the heart after MI.

Gdf5-deficient mice exhibit adverse infarct remodeling. Tetrazolium staining of heart sections at 1 day after MI showed no difference in ischemic area between Gdf5-KO and WT mice. Infarct area at 7 days after MI also did not differ between Gdf5-KO and WT mice. However, by 28 days after MI, morphometry revealed a 42% greater infarct area in Gdf5-KO mice as compared with WT control subjects (Table 1). At 28 days after MI, ventricular weight to body weight ratio was elevated by 9% in Gdf5-KO as compared with WT (Fig. 2). At this time point, hearts from Gdf5-KO mice exhibited a 30% increase in thinning of the infarcted LV and transmural infarct expansion (Table 1). The full thickness extent of the infarct (i.e., its transmurality) at 28 days after MI, as quantified by 2 different formulae (13), was significantly greater in Gdf5-KO as compared with WT mice (Table 1). Finally, quantification of dilation and thinning of the infarct wall (13) revealed 156% greater infarct expansion (infarct topography and area without additional necrosis) in Gdf5-KO mice (Table 1). These data indicate that Gdf5 plays an important role in preventing infarct wall thinning, cardiac dilation, and infarct expansion.

Gdf5-deficient mice exhibit impaired cardiac function after MI. Terminal hemodynamic studies at 28 days after MI revealed expected reductions in measures of cardiac

JACC Vol. 55, No. 2, 2010
January 12, 2010:135–43

Table 1 Morphometry Data

Parameters	WT	KO	p Value
Infarct area, 7 days after MI	34.95 ± 5.68	31.97 ± 4.74	0.403
Infarct area, 28 days after MI	31.73 ± 2.98	45.10 ± 4.25	0.013
Infarct thickness, 28 days after MI	0.64 ± 0.05	0.45 ± 0.04	0.007
Degree of transmurality (%), 28 days after MI	61.89 ± 6.59	83.13 ± 3.03	0.009
Area subtended by infarct (%), 28 days after MI	61.06 ± 3.87	87.28 ± 2.72	<0.0001
Expansion index, 28 days after MI	0.70 ± 0.10	1.79 ± 0.35	<0.003

Infarct area ([infarct area/total left ventricle (LV) area] × 100) was calculated at 7 days for growth differentiation factor 5 (Gdf5)-knockout (KO) and wild-type (WT) (n = 7 each) mice and 28 days for Gdf5-KO (n = 16) and WT mice (n = 19). Infarct thickness was calculated by averaging thickness of the infarct over 5 equally spaced locations and dividing by thickness of the noninfarcted LV measured at mid-septum. Transmurality was defined as infarct length touching the epicardium divided by total infarct length. Area subtended by the infarct was determined by the formula: infarct area/entire LV area subtended by outer infarct margin. Expansion index was calculated as described in the Results section. All data are mean ± SEM. Analyses were by Student *t* test.
MI = myocardial infarction.

Table 2 Hemodynamic Data

Parameters (28 Days After MI)	WT (n ≥ 16)	KO (n = 18)	p Value
HR (beats/min)	565 ± 15	545 ± 12	0.298
SBP (mm Hg)	96 ± 3.5	82 ± 2.7	0.004
DBP (mm Hg)	78 ± 3.4	68 ± 2.4	0.026
MAP (mm Hg)	84 ± 3.4	73 ± 2.5	0.013
LVSP (mm Hg)	101 ± 4.1	85 ± 3.0	0.004
+dP/dt (mm Hg/s)	4,627 ± 179	3,812 ± 135	<0.001
−dP/dt (mm Hg/s)	4,531 ± 173	3,802 ± 151	0.003

Data were analyzed by Student *t* test. All data are mean ± SEM.
DBP = aortic diastolic blood pressure; ±dP/dt = peak first derivatives of change in left ventricular pressure/time; HR = heart rate; LVSP = peak left ventricular systolic pressure; MAP = mean aortic blood pressure; SBP = aortic systolic blood pressure; other abbreviations as in Table 1.

function in LAD-ligated Gdf5-KO and WT mice as compared with their respective sham-operated control subjects (data not shown). However, within LAD-ligated groups, Gdf5-KO mice displayed significantly greater reductions in indexes of cardiac function than their WT control subjects (Table 2). In sham control subjects, parameters of cardiac function did not differ between Gdf5-KO and WT mice. However, mean arterial pressure was somewhat lower in Gdf5-KO (77 ± 2.5, n = 10) versus WT (92 ± 3.9, n = 12) mice ($p < 0.05$). Although cardiac function of Gdf5-KO and WT did not differ at 8 days after MI, it was significantly reduced in Gdf5-KO mice at 14 days after MI (Supplementary Table B).

Differential activation of p38-MAPK and Smad 1/5/8 in Gdf5-KO and WT hearts. As known downstream mediators of BMP or Gdf5 signaling in other tissues (1,2,16), the activation (i.e., phosphorylation) of Smad 1/5/8 and p38-MAPK was first examined by Western blot of heart lysates from WT mice. Although total Smad 1/5/8 and p38-MAPK protein levels did not change, Smad 1/5/8 phosphorylation increased slightly at 14 days after MI, and p38-MAPK phosphorylation was decreased at both 7 and 14 days after MI (Fig. 3A). We next compared expression and phosphorylation of these signaling proteins in the hearts of Gdf5-KO and -WT mice at 7 days after MI. Although total Smad 1/5/8 and p38-MAPK levels did not differ between Gdf5-KO and WT hearts, phosphorylation of Smad 1/5/8 was increased approximately 3-fold in Gdf5-KO hearts, whereas phosphorylation of p38-MAPK was reduced approximately 80% (Fig. 3B). Increased phosphorylated Smad 1/5/8 in Gdf5-KO hearts was predominantly present within the infarct area (Supplementary Fig. 2). At this time point, activated levels of ERK1/2 and c-jun N-terminal kinase did not differ between Gdf5-KO and WT mice (data not shown). These experiments revealed that Gdf5 deficiency results in a significant and seemingly selective reduction in p38-MAPK signaling after MI.

Gdf5 deficiency increased collagen gene expression and fibrosis after MI. Signaling via p38-MAPK is known to suppress collagen type I, alpha-1 (Col1a1) and collagen type III, and alpha-1 (Col3a1) gene transcription in cardiac cells (17) and to reduce cardiac fibrosis after MI (18). Because Gdf5-KO mice manifest reduced p38-MAPK phosphorylation after MI, we next examined collagen gene expression and fibrosis in WT and Gdf5-KO mice. In WT mice, Col1a1

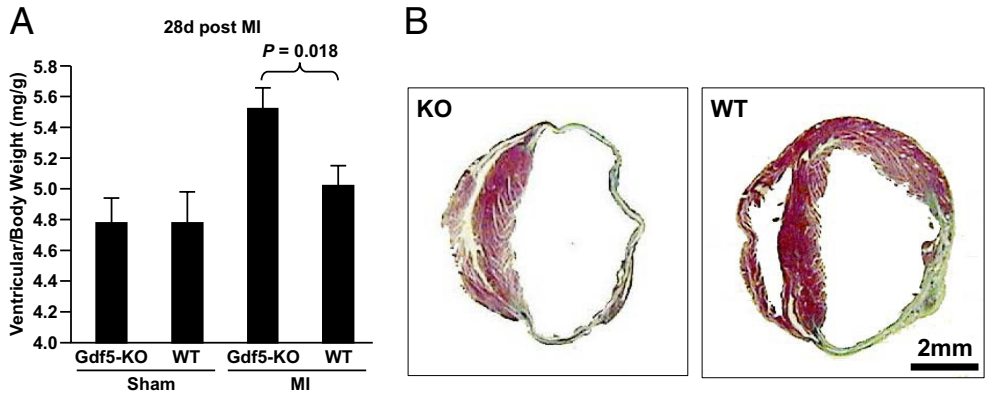

Figure 2 Gdf5-Deficiency Adversely Affects Cardiac Remodeling After MI

(A) Ventricle to body weight ratios at 28 days after MI or sham. **(B)** Representative trichrome-stained sections of 28 days after MI hearts.
Data are mean ± SE. Analysis was by 2-way ANOVA followed by Bonferroni test. KO = knockout; WT = wild-type; other abbreviations as in Figure 1.

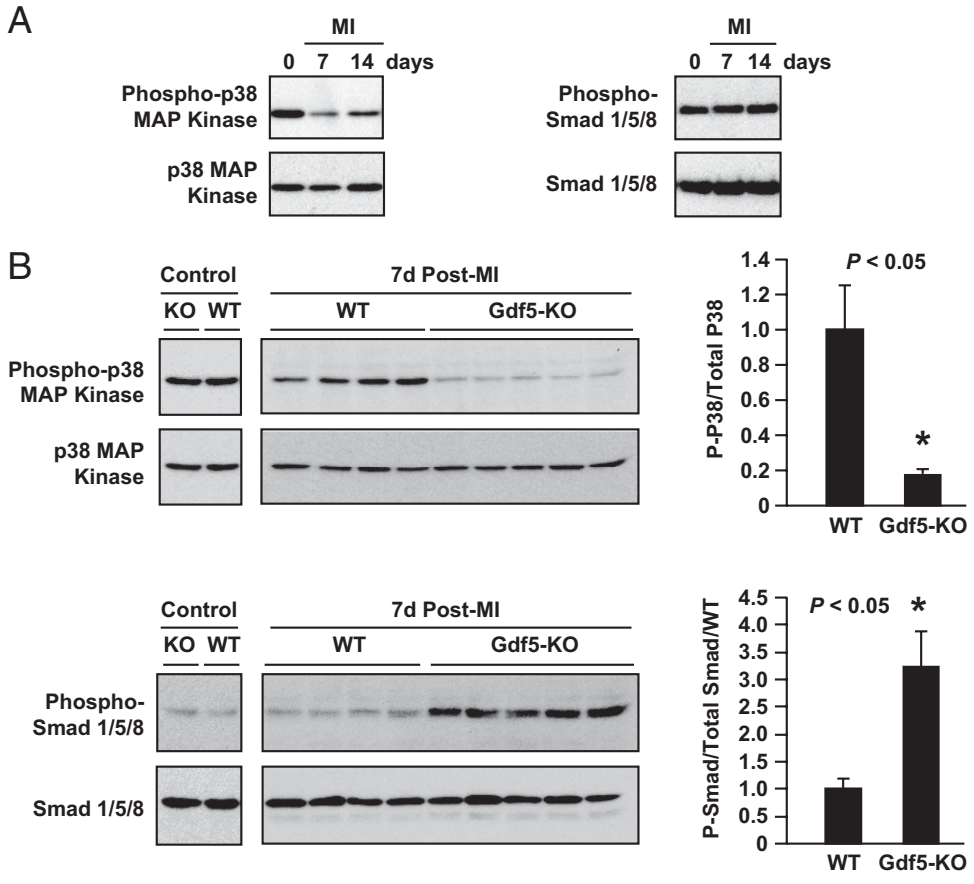

Figure 3 Gdf5-Deficiency Alters Smad and p38 Signaling After MI

Phosphorylated and total p38 mitogen-activated protein kinase (MAPK) and Smad 1/5/8 levels in hearts of **(A)** WT mice after MI and **(B)** nonsurgical and 7 days after MI Gdf5-KO and WT mice. **Right panels** show densitometric ratios of phosphorylated and total p38-MAPK and Smad 1/5/8 at 7 days after MI. **Left panels** show that p38-MAPK and Smad 1/5/8 levels are similar in nonsurgical Gdf5-KO and WT control subjects. *p < 0.05 versus WT. Abbreviations as in Figures 1 and 2.

(Fig. 4A) and Col3a1 (Fig. 4B) mRNA levels in the infarct zone were elevated 19- and 16-fold, respectively, above sham-operated control subjects at 7 days after MI and 49- and 34-fold, respectively, at 14 days after MI. In Gdf5-KO mice, Col1a1 and Col3a1 mRNA levels were an additional 2.6- and 2.2-fold higher than in WT hearts at the 7-day time point. By 14 and 28 days after MI, this difference was no longer apparent, because Col1a1 and Col3a1 levels were similarly elevated in Gdf5-KO and WT mice versus sham. Of note, there were no differences in matrix metalloproteinase (MMP)-9 and MMP-2 levels between Gdf5-KO and WT hearts at 7 and 28 days after MI (Supplementary Fig. 3). Fibrosis was 46% greater in Gdf5-KO mice hearts, compared with WT mice, after MI (Fig. 4C). These studies showed that Gdf5 deficiency results in increased Col1a1 and Col3a1 mRNA expression and fibrosis after MI.

Gdf5 deficiency reduced the numbers of myocardial vessels after MI. Coronary artery occlusion is known to remodel the myocardial vasculature (19,20), and expression of phosphorylated p38-MAPK after MI has been correlated with vascular density and inversely correlated with infarct area (18). Accordingly, we examined arterial density in Gdf5-KO mice with smooth muscle (SM)-alpha-actin to identify muscular precapillary vessels. In the infarct region (infarct and border area), the number of SM-alpha-actin–stained vessels was reduced by 57% in Gdf5-KO hearts as compared with WT (Fig. 5), whereas the number of these vessels in noninfarcted regions did not differ. Similarly, in sham-operated control subjects, the number of SM-alpha-actin–stained cardiac vessels did not differ between Gdf5-KO and WT mice. At 14 days after MI, ID1 expression did not differ between the Gdf5-KO and WT mice (Supplementary Fig. 4). These observations showed that Gdf5 deficiency results in reduced numbers of muscular myocardial arteries, an effect independent of ID1 but consistent with reduced p38-MAPK signaling.

Gdf5 improved cardiomyocyte survival and increased expression of anti-apoptotic genes via Smad signaling. Because less viable myocardium was ultimately observed in Gdf5-KO mice at 28 days after MI (Fig. 2, Table 1), we also explored whether Gdf5 has effects on cardiomyocyte survival. In a cell culture model of serum-deprivation–induced apoptosis (21), the number of TUNEL-positive nuclei was reduced by 79% in rGdf5-treated cells (Fig. 6A). To identify putative mechanisms, we examined the mRNA

JACC Vol. 55, No. 2, 2010
January 12, 2010:135–43

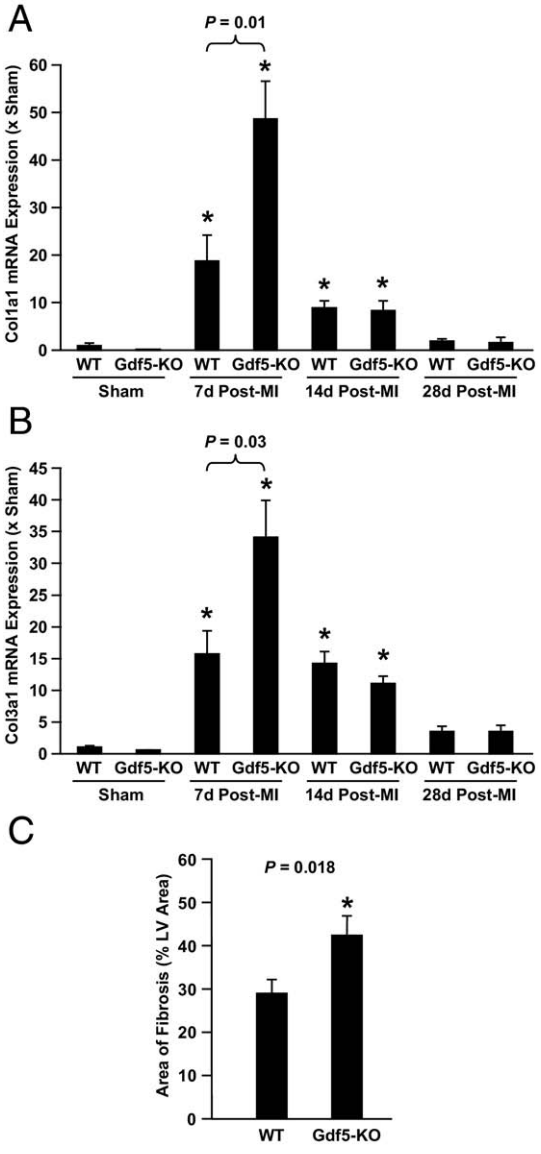

Figure 4 **Gdf5-Deficiency Increases Expression of Col1a1 and Col3a1 mRNA Levels and Cardiac Fibrosis After MI**

Real-time quantification of **(A)** Col1a1 and **(B)** Col3a1 mRNA levels in the infarct zones of hearts after MI. All data were normalized to Gapdh mRNA and sham control subjects and are given as mean ± SEM; n = 3 mice for each **bar** in sham, and n = 6 to 7 for each **bar** in post-MI. Data were compared by 1-way ANOVA followed by *t* test for multiple comparisons. All post-MI expression levels are higher than sham control subjects. *p < 0.001. **(C)** Area of fibrosis was calculated on trichrome-stained sections of hearts at 28 days after MI. Data are mean ± SEM. Abbreviations as in Figures 1 and 2.

levels of Bcl-xL, Bcl2, and Bax. The pro-survival effect of rGdf5 was accompanied by 53% and 138% increases in expression of the anti-apoptotic genes Bcl2 and Bcl-xL, respectively (Fig. 6B), with no change in the expression of the pro-apoptotic gene Bax. Of note, these effects of rGdf5 were also observed in the absence of an apoptotic insult (i.e., in serum-stimulated cardiomyocytes). These data suggest that Gdf5 might confer cardiomyocyte survival by elevating expression of Bcl2 and Bcl-xL.

To explore signaling mechanisms mediating the anti-apoptotic effects of rGdf5 in neonatal cardiomyocytes, we employed RNAi against Smad4, which is essential for Smad 1/5/8 signaling, and p38 MAPK. The RNAi to Smad4 decreased endogenous Smad4 (Fig. 7A) and blocked rGdf5-induced expression of Bcl-xL (Fig. 7B) and suppression of apoptosis (Fig. 7C). These effects were not observed with RNAi against p38-MAPK (Mapk14) (data not shown). Consistent with our in vitro findings, Gdf5-KO mice hearts showed increased apoptosis and decreased Bcl2 and Bcl-xL expression in the peri-infarct areas at 4 days after MI, compared with WT mice (Fig. 8).

Gdf5 induces p38-MAPK phosphorylation in cardiac fibroblasts. To examine whether rGdf5 activates p38-MAPK, cardiac fibroblasts and cardiomyocytes were treated with rGdf5. Phosphorylation of p38-MAPK was rapidly induced in cardiac fibroblasts treated with rGdf5 (Fig. 6C), with

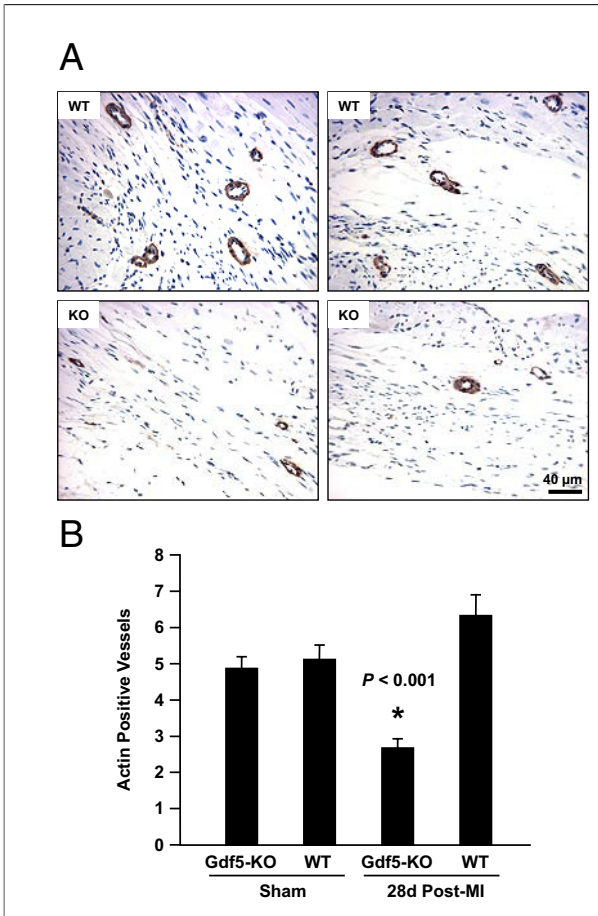

Figure 5 **Gdf5-Deficiency Reduces Abundance of Muscularized Myocardial Arteries After MI**

Sections were immunostained for smooth muscle-alpha-actin, and only stained vessels of 15 to 100 μm diameter were counted under a light microscope (40× objective) and averaged for each section. Vessels were counted in the anterior wall, including in normal tissue for sham, and in the infarct and border zones for LAD-ligated hearts. Data were analyzed by 2-way ANOVA ($p < 0.05$) followed by Bonferroni test. **(A)** Representative sections from the peri-infarct **(left panels)** and infarct **(right panels)** areas of the post-MI Gdf5-KO and WT hearts are shown. **(B)** Data are plotted as number of vessels/microscopic field and **bars** represent mean ± SEM. Abbreviations as in Figures 1 and 2.

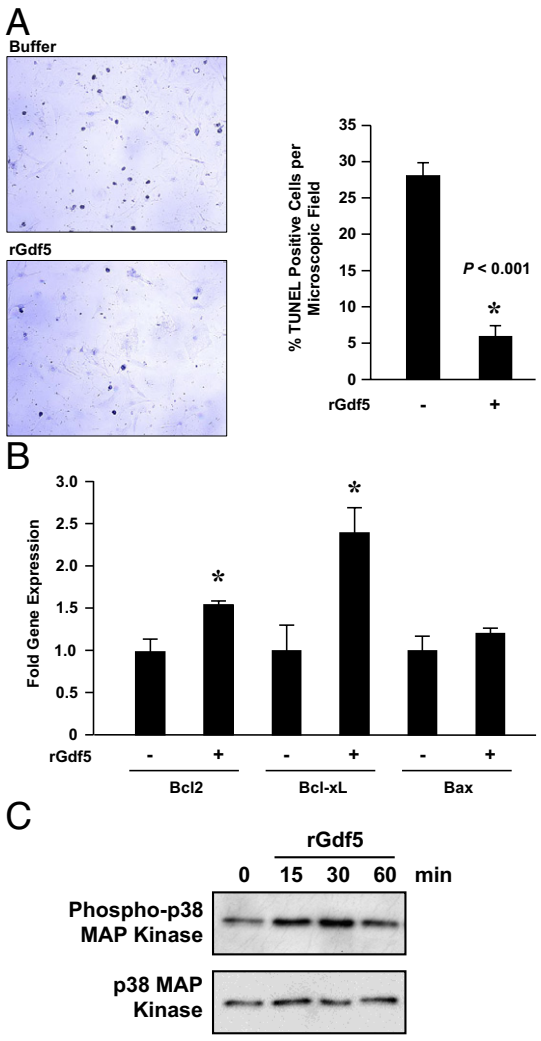

Figure 6 **Recombinant Gdf5 Improves Survival of Neonatal Cardiomyocytes and Induces p38-MAPK Phosphorylation in Cardiac Fibroblasts**

(A) Cardiomyocytes apoptosis was determined by terminal deoxynucleotidyl transferase (TdT)-mediated dUTP nick end labeling (TUNEL) labeling after 48 h of serum-free culture supplemented with rGdf5 or buffer. Data shown are representative of 3 independent experiments. **(B)** Quantitative real-time reverse-transcriptase polymerase chain reaction show elevated expression of Bcl2 and Bcl-xL in Gdf5-treated cells. Gene expression data were normalized to Gapdh and calculated as fold change versus buffer-treated control subjects *p < 0.05. **(C)** The rGdf5 induces phosphorylation of p38-MAPK in mouse cardiac fibroblasts. Abbreviations as in Figures 1 and 3.

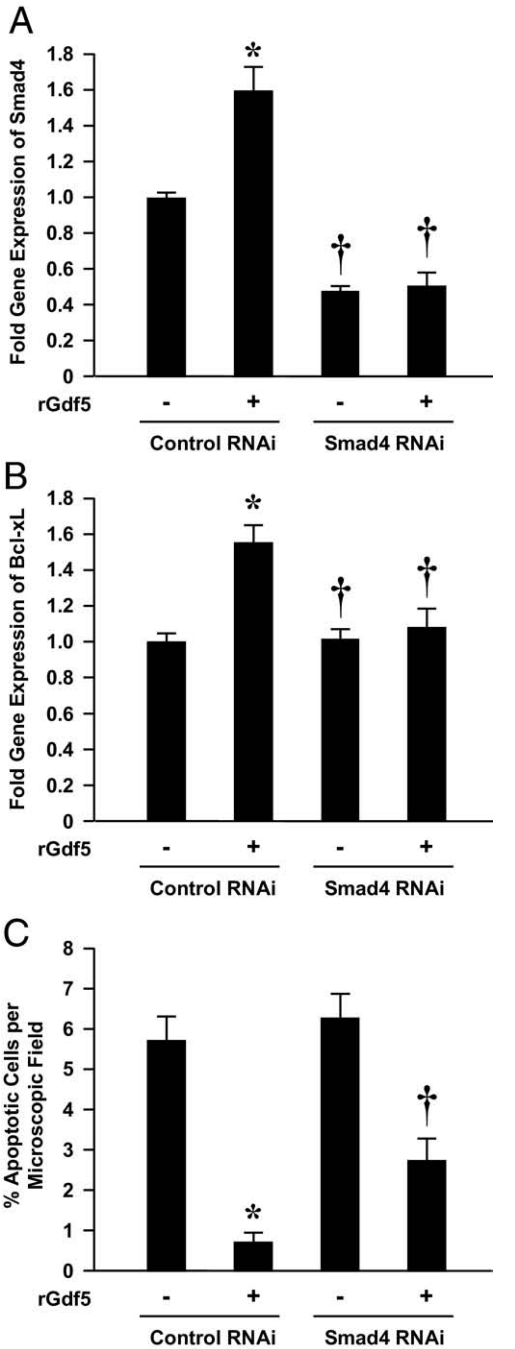

Figure 7 **Smad4 RNAi Ablates Gdf5 Induction of Bcl-xL and Suppression of Apoptosis in Neonatal Cardiomyocytes**

(A) Smad4 ribonucleic acid interference (RNAi) decreases Smad4 mRNA levels in neonatal cardiomyocytes. *p < 0.05 versus other treatments; †p < 0.001 versus control RNAi; n = 3/treatment. **(B)** Smad4 RNAi ablates rGdf5 induction of Bcl-xL mRNA. *p < 0.03 versus other treatments; †p < 0.05 versus buffer-treated control RNAi; n = 3/treatment. **(C)** Neonatal cardiomyocyte were transfected with Smad4 or control RNAi, and apoptosis was determined by caspase 3 immunostaining after 48 h of serum free culture with rGdf5 or buffer. *p < 0.001 versus buffer-treated control RNAi; †p = 0.007 versus Gdf5-treated control RNAi; n = 10 microscopic fields/treatment. Abbreviations as in Figures 1.

total p38-MAPK protein levels remaining unchanged. Of interest, activation of p38-MAPK was not observed in rGdf5-treated cardiomyocytes.

Discussion

Although some BMPs had been studied in cardiac development, their role in repair of the adult heart had not. We now show that Gdf5 (a.k.a., BMP14) is expressed in the adult mouse heart and that its levels are elevated after 7 days after MI. We further show that the receptors through which Gdf5 transduces its signals (3) are also expressed. More

JACC Vol. 55, No. 2, 2010
January 12, 2010:135–43

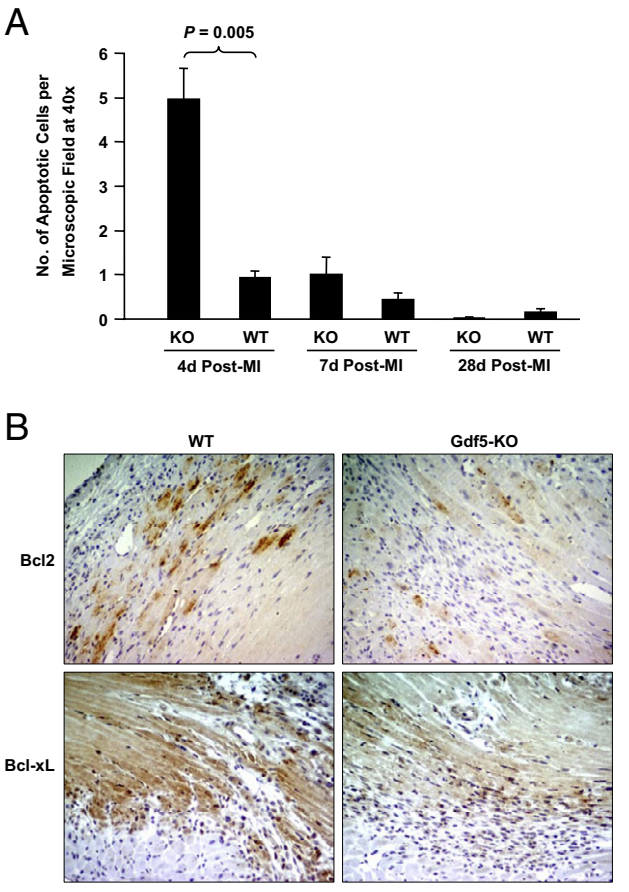

Figure 8 **Gdf5-KO Mice Exhibit Increased Apoptosis and Reduced Expression of Bcl2 and Bcl-xL After MI**

(A) Sections were immunostained for activated caspase-3. Apoptotic cells were counted in the peri-infarct areas of post-MI hearts under a light microscope (40× objective) and averaged for each section. **(B)** Post-MI heart sections were immunostained for Bcl2 and Bcl-xL. In Gdf5-KO mice, expression of these genes was lesser than the WT hearts after MI. Abbreviations as in Figures 1 and 2.

importantly, we are the first to show that the absence of this BMP results in impaired cardiac repair after MI, as manifest by increased indexes of post-healing infarct scar expansion, increased cardiomyocyte apoptosis, decreased vascular density, and accelerated functional deterioration in Gdf5-KO mice. Finally, our data suggest that the increased expression of Gdf5 after MI serves to improve cardiac repair by Smad-dependent reduction in cardiomyocyte apoptosis, enhanced p38-MAPK phosphorylation in cardiac fibroblasts, suppression of collagen expression and fibrosis, and preservation of vascular density. Together, these findings enhance our understanding of the mechanisms and importance of the transforming growth factor-beta super family in healing and repair after MI (22).

Hearts from Gdf5-KO mice exhibited increased ventricle/body weight ratio, infarct area, LV wall thinning, transmural infarct expansion, and cardiac dilation and thinning. The Gdf5-KO mice also displayed worse hemodynamic parameters after MI. Together these morphometric and functional studies indicate impaired cardiac repair and function in Gdf5-KO mice. To examine molecular causes underlying this phenotype, p38-MAPK and Smad 1/5/8 phosphorylation were studied in post-MI hearts. Compared with WT, Gdf5-KO mice exhibited decreased p38-MAPK phosphorylation and increased Smad 1/5/8 phosphorylation. Although the unexpected increase in phosphorylated Smad 1/5/8 in the infarct area might be due to dysregulated expression of other BMPs or inhibitory Smads, the documented effects of Gdf5 deficiency on post-healing infarct scar expansion, apoptosis, vascular density, cardiac function, and fibrosis are entirely consistent with the decreased p38-MAPK phosphorylation observed in Gdf5-KO mice.

Indeed, several lines of evidence suggest that the phenotype of Gdf5-deficient mice might be partly due to reduced p38-MAPK signaling. First, normalization of reduced p38-MAPK phosphorylation in post-MI hearts has been shown to reduce infarct area, increase vascular density, improve cardiac function, and decrease cardiac fibrosis and apoptosis (18). Second, cardiomyocyte-specific p38-MAPK deletion produced massive cardiac fibrosis and elevated collagen expression after pressure overload (23). Third, p38-MAPK phosphorylation is known to suppress Col1a1 and Col3a1 transcription in cardiomyocytes (17).

Whether directly or indirectly dependent on p38-MAPK signaling, our findings of reduced numbers of muscular arteries in the Gdf5-KO heart after LAD ligation are consistent with an important role for Gdf5 in tissue vascularity. The Gdf5-KO mice have previously been shown to have a defect in revascularization after tendon injury (11), and rGdf5 is known to confer angiogenesis in chick chorioallantoic membrane and rabbit cornea (8). The importance of this "vascular" effect on the post-MI phenotype of Gdf5-KO mice is likely to be high. Others have shown loss of coronary arteries after MI, followed by a gradual increase in capillary and arteriolar densities over 3 weeks (19). This is believed to enhance blood flow, reduce infarct area, and contribute to cardio-protection in hypoxia-preconditioned ischemic hearts (19). Other studies supporting post-MI angiogenesis in mice include increased perfusion (20) and improved LV function after therapeutic angiogenesis (24). As such, we believe that the decreased infarct-zone vascularity of Gdf5-KO mice is a major contributor to the documented increases in infarct thinning and expansion. Further studies will be needed to explore what role, if any, is played by Gdf5 on the abundance or recruitment of circulating endothelial progenitors, cells known to participate in angiogenesis and repair after MI (25,26).

The Gdf5 is a pleiotropic BMP that is also known to confer anti-apoptotic and pro-apoptotic effects on different cells (6,9). Here, we show that cardiomyocyte survival in rGdf5-treated cells and in post-MI hearts is associated with increased expression of Bcl-xL and Bcl2, which are potent inhibitors of apoptosis. The Bcl2 gene transfer has also been shown to improve post-MI repair by reducing cardiomyocyte apoptosis (27). In rat cardiomyocytes, BMP2 improved cell survival by increasing Bcl-xL but not Bcl2 mRNA levels (21). Finally, rGdf5 induced rapid p38-MAPK phosphor-

ylation in cultured neonatal cardiac fibroblasts but not in cardiomyocytes. Together, these data suggest complementary mechanisms through which the Gdf5 deficiency might have adversely affected repair after MI.

Our isolated finding of a mildly reduced systemic blood pressure in noninfarcted (i.e., sham-operated) Gdf5-KO mice as compared with WT mice might be related to the lower body weight and shorter limbs of Gdf5-KO mice. Alternatively, this difference might suggest an additional role for Gdf5 in vascular function and blood pressure. Because no structural or functional differences could be detected between the hearts of healthy Gdf5-KO and WT mice, additional studies will be needed to explore the basis of the blood pressure observation.

Conclusions

We have shown that Gdf5 and its receptors are expressed in adult mouse heart and that the Gdf5 levels are elevated after MI. The Gdf5-deficiency impaired cardiac repair after MI; a phenotype associated with reduced p38-MAPK phosphorylation, elevated Col1a1 and Col1a3 mRNA levels, increased fibrosis, enhanced apoptosis, and reduced vascularization of the LV wall after MI. Having said this, Gdf5 is only one of several molecules involved in post-MI repair. Furthermore, uninjured Gdf5-KO mice survive without pertinent abnormalities. Accordingly, overlapping expression of other BMPs or growth factors might be partially compensating for the loss of Gdf5 in the KO model. Despite this possibility, the perturbations caused by Gdf5 deficiency have promoted the initiation of irreversible events that led to decreased vascularity and greater loss of myocardium in Gdf5-KO mice. Our results indicate that endogenous levels of Gdf5 in particular and BMPs in general influence cardiac repair after injury or ischemia. In addition, our study supports the potential use of Gdf5-based therapies to improve repair and reduce progressive loss of cardiomyocytes after infarction.

Reprint requests and correspondence: Dr. Syed H. E. Zaidi, Division of Cardiology, Department of Medicine, University of Toronto and University Health Network, 101 College Street, TMDT East Tower, Room 3-910, Toronto, Ontario M5G 1L7, Canada. E-mail: syed.zaidi@uhnres.utoronto.ca.

REFERENCES

1. Nakamura K, Shirai T, Morishita S, Uchida S, Saeki-Miura K, Makishima F. p38 mitogen-activated protein kinase functionally contributes to chondrogenesis induced by growth/differentiation factor-5 in ATDC5 cells. Exp Cell Res 1999;250:351–63.
2. Coleman CM, Tuan RS. Functional role of growth/differentiation factor 5 in chondrogenesis of limb mesenchymal cells. Mech Dev 2003;120:823–36.
3. Nishitoh H, Ichijo H, Kimura M, et al. Identification of type I and type II serine/threonine kinase receptors for growth/differentiation factor-5. J Biol Chem 1996;271:21345–52.
4. Storm EE, Huynh TV, Copeland NG, Jenkins NA, Kingsley DM, Lee SJ. Limb alterations in brachypodism mice due to mutations in a new member of the TGF beta-superfamily. Nature 1994;368:639–43.
5. Coleman CM, Loredo GA, Lo CW, Tuan RS. Correlation of GDF5 and connexin 43 mRNA expression during embryonic development. Anat Rec A Discov Mol Cell Evol Biol 2003;275:1117–21.
6. Sullivan AM, O'Keeffe GW. The role of growth/differentiation factor 5 (GDF5) in the induction and survival of midbrain dopaminergic neurones: relevance to Parkinson's disease treatment. J Anat 2005;207:219–26.
7. Chen X, Zankl A, Niroomand F, et al. Upregulation of ID protein by growth and differentiation factor 5 (GDF5) through a smad-dependent and MAPK-independent pathway in HUVSMC. J Mol Cell Cardiol 2006;41:26–33.
8. Yamashita H, Shimizu A, Kato M, et al. Growth/differentiation factor-5 induces angiogenesis in vivo. Exp Cell Res 1997;235:218–26.
9. Nakahara T, Tominaga K, Koseki T, et al. Growth/differentiation factor-5 induces growth arrest and apoptosis in mouse B lineage cells with modulation by Smad. Cell Signal 2003;15:181–7.
10. Zeng Q, Li X, Beck G, Balian G, Shen FH. Growth and differentiation factor-5 (GDF-5) stimulates osteogenic differentiation and increases vascular endothelial growth factor (VEGF) levels in fat-derived stromal cells in vitro. Bone 2007;40:374–81.
11. Chhabra A, Tsou D, Clark RT, Gaschen V, Hunziker EB, Mikic B. GDF-5 deficiency in mice delays Achilles tendon healing. J Orthop Res 2003;21:826–35.
12. Ohta K, Nakajima T, Cheah AY, et al. Elafin-overexpressing mice have improved cardiac function after myocardial infarction. Am J Physiol Heart Circ Physiol 2004;287:H286–92.
13. Hochman JS, Choo H. Limitation of myocardial infarct expansion by reperfusion independent of myocardial salvage. Circulation 1987;75:299–306.
14. Dubey RK, Gillespie DG, Mi Z, Jackson EK. Exogenous and endogenous adenosine inhibits fetal calf serum-induced growth of rat cardiac fibroblasts: role of A2B receptors. Circulation 1997;96:2656–66.
15. Li RK, Mickle DA, Weisel RD, Zhang J, Mohabeer MK. In vivo survival and function of transplanted rat cardiomyocytes. Circ Res 1996;78:283–8.
16. Upton PD, Long L, Trembath RC, Morrell NW. Functional characterization of bone morphogenetic protein binding sites and Smad1/5 activation in human vascular cells. Mol Pharmacol 2008;73:539–52.
17. Ambrosino C, Iwata T, Scafoglio C, Mallardo M, Klein R, Nebreda AR. TEF-1 and C/EBPbeta are major p38alpha MAPK-regulated transcription factors in proliferating cardiomyocytes. Biochem J 2006;396:163–72.
18. Tenhunen O, Soini Y, Ilves M, et al. p38 kinase rescues failing myocardium after myocardial infarction: evidence for angiogenic and anti-apoptotic mechanisms. Faseb J 2006;20:1907–9.
19. Sasaki H, Fukuda S, Otani H, et al. Hypoxic preconditioning triggers myocardial angiogenesis: a novel approach to enhance contractile functional reserve in rat with myocardial infarction. J Mol Cell Cardiol 2002;34:335–48.
20. Meoli DF, Sadeghi MM, Krassilnikova S, et al. Noninvasive imaging of myocardial angiogenesis following experimental myocardial infarction. J Clin Invest 2004;113:1684–91.
21. Izumi M, Fujio Y, Kunisada K, et al. Bone morphogenetic protein-2 inhibits serum deprivation-induced apoptosis of neonatal cardiac myocytes through activation of the Smad1 pathway. J Biol Chem 2001;276:31133–41.
22. Bujak M, Frangogiannis NG. The role of TGF-beta signaling in myocardial infarction and cardiac remodeling. Cardiovasc Res 2007;74:184–95.
23. Nishida K, Yamaguchi O, Hirotani S, et al. p38alpha mitogen-activated protein kinase plays a critical role in cardiomyocyte survival but not in cardiac hypertrophic growth in response to pressure overload. Mol Cell Biol 2004;24:10611–20.
24. Hao X, Mansson-Broberg A, Grinnemo KH, et al. Myocardial angiogenesis after plasmid or adenoviral VEGF-A(165) gene transfer in rat myocardial infarction model. Cardiovasc Res 2007;73:481–7.
25. Qin G, Ii M, Silver M, et al. Functional disruption of alpha4 integrin mobilizes bone marrow-derived endothelial progenitors and augments ischemic neovascularization. J Exp Med 2006;203:153–63.
26. Jujo K, Ii M, Losordo DW. Endothelial progenitor cells in neovascularization of infarcted myocardium. J Mol Cell Cardiol 2008;45:530–44.
27. Chatterjee S, Stewart AS, Bish LT, et al. Viral gene transfer of the antiapoptotic factor Bcl-2 protects against chronic postischemic heart failure. Circulation 2002;106:I212–7.

Key Words: collagen gene expression ■ growth differentiation factor 5 ■ mitogen-activated protein kinase ■ myocardial infarction.

APPENDIX

For Supplementary Figures 1 to 4 and Supplementary Tables A and B, please see the online version of this article.